

Review Article

Molecular-Beam Epitaxially Grown MgB₂ Thin Films and Superconducting Tunnel Junctions

Jean-Baptiste Laloë,¹ Tae Hee Kim,² and Jagadeesh S. Moodera¹

¹Francis Bitter Magnet Laboratory, MIT, 160 Albany Street, Cambridge, MA 02139, USA

²Department of Physics, Ewha Womans University, 11-1 Dae Hyun-Dong, Soe Dae Moon-Gu, Seoul 120-750, Republic of Korea

Correspondence should be addressed to Jean-Baptiste Laloë, laloe@mit.edu

Received 2 February 2011; Accepted 4 April 2011

Academic Editor: Victor V. Moshchalkov

Copyright © 2011 Jean-Baptiste Laloë et al. This is an open access article distributed under the Creative Commons Attribution License, which permits unrestricted use, distribution, and reproduction in any medium, provided the original work is properly cited.

Since the discovery of its superconducting properties in 2001, magnesium diboride has generated terrific scientific and engineering research interest around the world. With a T_C of 39 K and two superconducting gaps, MgB₂ has great promise from the fundamental point of view, as well as immediate applications. Several techniques for thin film deposition and heterojunction formation have been established, each with its own advantages and drawbacks. Here, we will present a brief overview of research based on MgB₂ thin films grown by molecular beam epitaxy coevaporation of Mg and B. The films are smooth and highly crystalline, and the technique allows for virtually any heterostructure to be formed, including all-MgB₂ tunnel junctions. Such devices have been characterized, with both quasiparticle and Josephson tunneling reported. MgB₂ remains a material of great potential for a multitude of further characterization and exploration research projects and applications.

Magnesium diboride has been readily available to purchase “over the counter” for more than half a century. However, it was not until early 2001 that a group of Japanese researchers announced their discovery that it was superconducting, with a T_C of 39 K [1]. This exciting discovery immediately attracted the attention of many research groups worldwide, and since then hundreds of research papers have been published on MgB₂ and MgB₂-based devices. The justification of this drive is obvious: MgB₂ is a simple binary compound, both elemental components of which are inexpensive, abundant, and nontoxic. It has a simple hexagonal crystal structure, and a robust lattice, shown in Figure 1. Perhaps most significantly, though, the high transition temperature signifies that MgB₂-based devices should reliably operate at temperatures of up to 20 or even 30 K, easily made possible by closed-cycle cryogenic compressors or liquefied neon, thus immediately eliminating the need for expensive liquid helium and the associated bulk infrastructure [2–4].

MgB₂ instantly drew interest from the health industry, and novel methods of synthesizing efficient superconducting wires (e.g., for magnetic resonance imaging (MRI) machines) were developed as early as 2003, and are continu-

ally being improved. The main manufacturing challenge here is concerned with the porosity of the compound, and the operational limit is the critical current density—the maximum current the threads can sustain while remaining in the superconducting state—of the wire. After developing new methods of pressing the source material into wires, multicore geometries and sintering treatments, several commercial companies now offer MgB₂ wires with good application potential.

In addition to this, the newly found superconductor would also present some novel physics explored by the research community. Particularly, it appeared at first very surprising that such a compound could become superconducting at such a high temperature. This prompted a wealth of research into the mechanism of superconductivity and Cooper pair formation in MgB₂, leading to the currently accepted explanation that MgB₂ presents two superconducting energy gaps. Simulations of the lattice and understanding of the electron bands indicate that the two gaps coexist in the two directions of the crystal lattice. At 4.2 K, the π -gap has a value of ~ 2.2 meV, and the large σ -gap has a value of ~ 7.1 meV [5–10]. The two gaps are coupled, and both

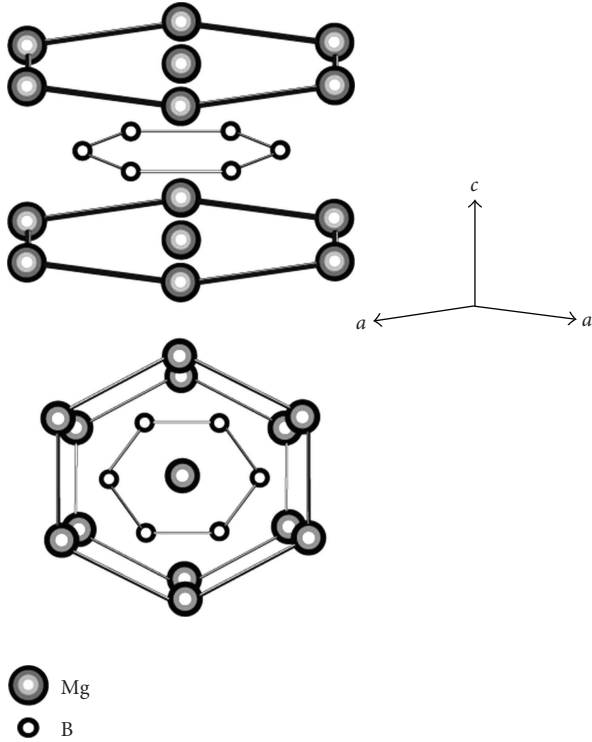


FIGURE 1: (From [1]) Crystal structure of MgB_2 , of the space group $P6/mmm$ (#191). MgB_2 is composed of interleaved Mg and B layers. © Nature publishing group.

close as the temperature increases to 39 K. Choi et al. [8] theoretically examined the origin and evolution of the two gaps on the Fermi surface of MgB_2 (Figure 2). The authors find that the crystal lattice (honeycomb planes of B atoms with Mg occupying the center of the hexagons in between B planes) is critical to electron bonding in the superconductor. Similarly to graphite, MgB_2 has strong σ bonds in the planes, and weak π bonds between the planes. The σ bonds are only partially occupied, resulting in strong Cooper pair formation confined to the planes of the lattice, the cause of the large σ band gap.

Furthermore, in 2009 the two gaps were theoretically predicted and experimentally found to behave in the two different superconducting regimes (type 1 and 2), providing yet another enigma and further research drive with this compound. Based on Bardeen-Cooper-Schrieffer (BCS) theory, Moshchalkov et al. [10] calculate the coherence lengths for the two gaps in MgB_2 , and find $\xi_\pi = 51$ nm, and $\xi_\sigma = 13$ nm, the former of which was in agreement with experimental vortex profile measurements [11]. The penetration depths, determined experimentally, were found to be $\lambda_\pi = 33.6$ nm and $\lambda_\sigma = 47.8$ nm [7]. The order parameter $\kappa = \lambda/\xi$ for each gap can then be calculated, resulting in the surprising finding that $\kappa_\pi < 1/\sqrt{2}$, and $\kappa_\sigma > 1/\sqrt{2}$. Thus, the two superconducting gaps (in the clean limit) are expected to behave according to both type 1 (π -gap) and type 2 (σ -gap) superconductivity, and the authors coin the term “type 1.5” superconductivity for MgB_2 . By studying the equilibrium vortex structure

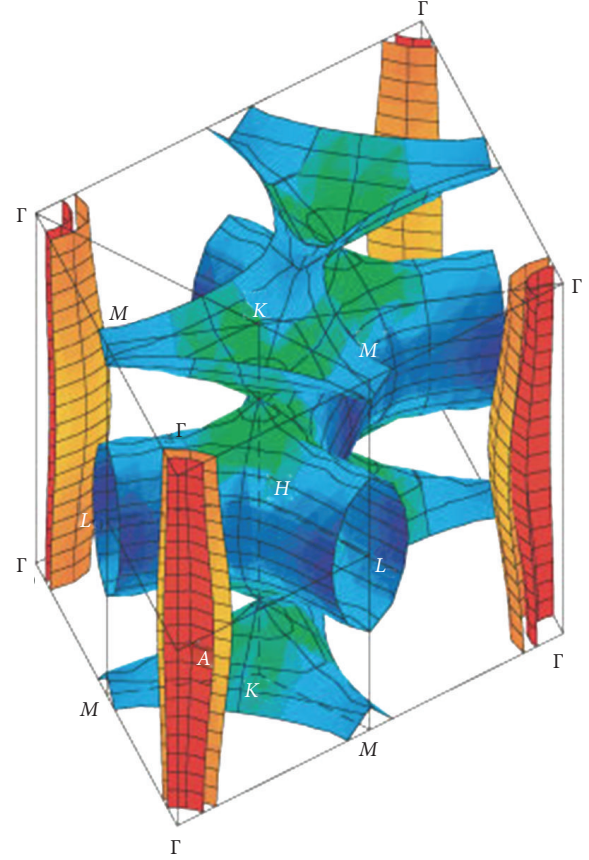


FIGURE 2: (From [8]) Calculated Fermi surface of MgB_2 , composed of four distinctive sheets. The σ sheets from the x, y orbitals of B are shown in red/orange (gap value ~ 7.1 meV), whereas the π sheets from the z orbitals of B are shown in blue/green (gap value ~ 2.2 meV). © Nature publishing group.

observed by Bitter decoration on MgB_2 crystals and comparing these results to theoretical predictions for this new type 1.5 regime, the authors confirm that their two-component model fits very well with the new superconductor.

As the material properties of MgB_2 became better established, researchers began to integrate it in potentially highly impactful devices such as tunnel junctions. Indeed tunnel junctions would shed light on transport and speed limitations of MgB_2 , and are the first step towards Josephson junctions and subsequent highly sensitive field sensors, again with possible operating temperatures above 20 K. A significant research effort into MgB_2 thin films ensued, and several growth methods were established.

Some initial reports described processes requiring annealing (of e.g., a Mg and B superlattice) after deposition to achieve superconductivity in thin films [12–18]. Some of these films exhibited good superconducting properties, but their surface roughness and off-stoichiometric composition was a serious drawback for multilayer devices. As-deposited superconducting films would allow for multilayers to be readily formed and would be greatly favorable for lithography. Some early researchers reported on as-grown

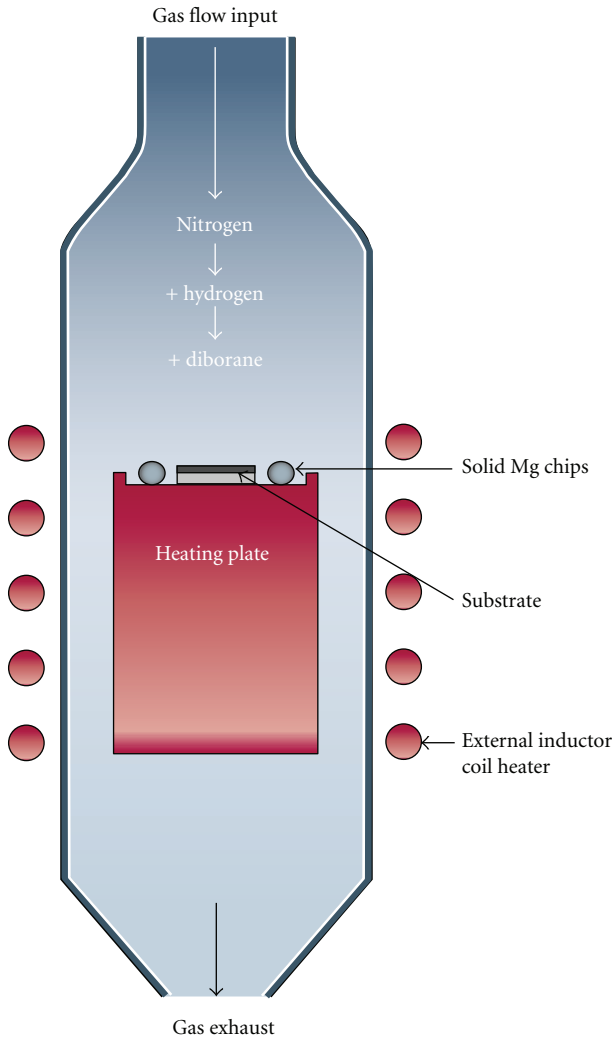


FIGURE 3: (From [22]): Schematic of the hybrid physical-chemical vapor deposition technique for growing epitaxial MgB_2 films. Vaporized Mg reacts with B from the flowing diborane gas, and an MgB_2 film condenses onto the substrate. ©Nature publishing group.

superconducting films, but these showed poor crystallinity [19, 20].

One deposition method which has been very successful and fruitful this past decade is the so-called hybrid physical-chemical vapor deposition developed by Zeng et al. [21] and Rowell [22]. This involves heating a substrate in the presence of Mg vapor while exposing the substrate to a flow of diborane gas, as schematically shown in Figure 3. A highly crystalline MgB_2 layer then grows very quickly on the substrate, as long as the gas flow remains. Layers grown by this method display excellent T_C and low resistivity comparable to annealed single crystals, accompanied by high critical current densities ($\sim 10^7 \text{ A}\cdot\text{cm}^{-2}$). A drawback of this deposition process (in addition to the requirement of poisonous diborane) is the challenge of depositing multiple layers or tunnel junctions without breaking the vacuum and thus risking contaminating the surface. Nevertheless,

this deposition technique has been a catalyst for MgB_2 thin film research around the world, with many dozens of projects and articles benefiting from these films (see, e.g., [23] and references therein), including Josephson junctions being successfully formed using Pb as a top electrode [24].

A second successful deposition method established (including in our group) by 2002, has been the coevaporation of Mg and B in a molecular beam epitaxy (MBE) chamber [19, 25]. Magnesium and boron have very different vapor pressures, requiring coevaporation of the two materials separately, Mg in a Knudsen cell (*k*-cell), and B from an electron beam (*e*-beam) source. In addition, B has a very high melting point and becomes very strained during rapid heating and cooling, sometimes breaking, leading to large fluctuations in the evaporation rate or even explosion of the source material.

MgB_2 thin film deposition was achieved on Si wafers in an ultrahigh vacuum chamber, with a base pressure of under 5×10^{-10} Torr. To promote lattice matching and avoid the formation of unwanted compounds such as silicon borides at the interface, a thin MgO buffer layer can be evaporated onto the heated clean Si (111) prior to MgB_2 growth. For MBE deposition of MgB_2 , the substrate temperature must be held above 250°C , and care must be taken regarding the fluxes, and the ratio of Mg and B fluxes. Mg has a very high vapor pressure, reaching 10^{-8} Torr by 185°C , and hence will fail to condense onto a hot substrate when evaporated alone. In the presence of B, though, the compound may form and deposit onto the substrate. It is typically the case that the quantity of Mg present during growth should be up to five-times greater than that of B, to avoid B-rich insulating films. The optimal flux ratio changes at each substrate temperature, thus forming a narrow window of suitable growth conditions. Using this method, though, it is possible to obtain highly oriented and very smooth films (roughness below 0.5 nm), as seen by a collection of X-ray characterization measurements shown in Figure 4.

Thin films grown by this method typically exhibit a transition temperature below 39 K, with thicker films (up to 200 nm thick) having a T_C of $34 \sim 37$ K. T_C is found to decrease with decreasing thickness, with 10 nm films becoming superconductive below ~ 22 K. This difference between the transition temperature of the bulk and thin films is caused by factors such as lower growth temperature, strain, oxygen contamination, and nonstoichiometry. Strain is a major factor in film growth and in the thin limit the region in the MgB_2 which is under considerable strain due to lattice mismatching will have a proportionally large effect on the film properties. Even if the lattice matching is close, as is the case with an oriented MgO buffer layer, interfacial effects will always be detrimental to the film's properties. Oxygen content and contamination is one other harmful occurrence to MgB_2 thin films, as Mg has a strong tendency to associate with any O_2 present during growth, forming MgO . This can result in some oxygen defects being trapped in the deposited film, depending on the growth conditions. By varying the background oxygen content during growth, Van Erven et al. [25] determined that films deposited in as little as 3×10^{-8} Torr of background oxygen exhibited

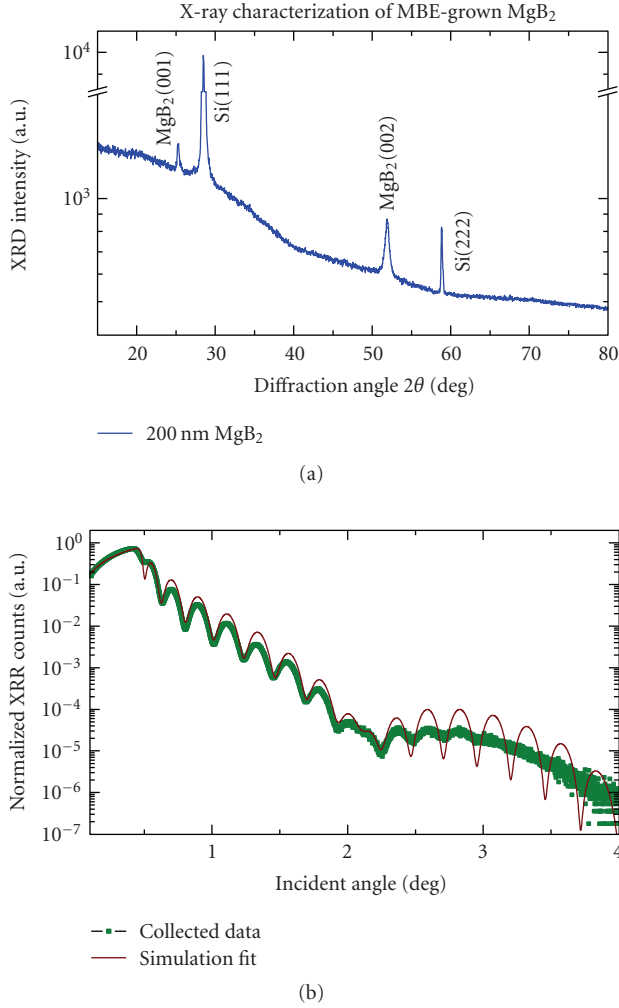


FIGURE 4: X-ray characterization of MBE-grown MgB₂: (a) X-ray diffraction of a 200 nm film, showing only the MgB₂(00 l) diffraction peaks in addition to substrate peaks; (b) Reflectivity scan of a MgB₂ thin film. The film thickness and roughness amplitude are extracted from the simulation fit to the data.

purely insulating behavior. Furthermore, stoichiometric films left uncapped but in an ultrahigh vacuum environment (6×10^{-10} Torr) for even thirty minutes started to show signatures of oxygen contamination, as studied with Auger electron spectroscopy (AES).

Perhaps more significant than the high-quality thin films which can be deposited by MBE, is the possibility of forming hetero-structures: in particular the ability to form tunnel junctions is a great advantage of this technique. Indeed, an as-deposited MgB₂ thin film in the chamber can immediately be capped with another material for protection prior to breaking of the vacuum. Furthermore, one can imagine and indeed achieve any combination of thin film devices into which MgB₂ can be integrated. The first device that comes to mind is naturally a tunnel junction—two conducting or superconducting layers separated by a thin insulating barrier. Tunnel junctions allow for the study of fundamental transport properties through the electrodes and the barrier

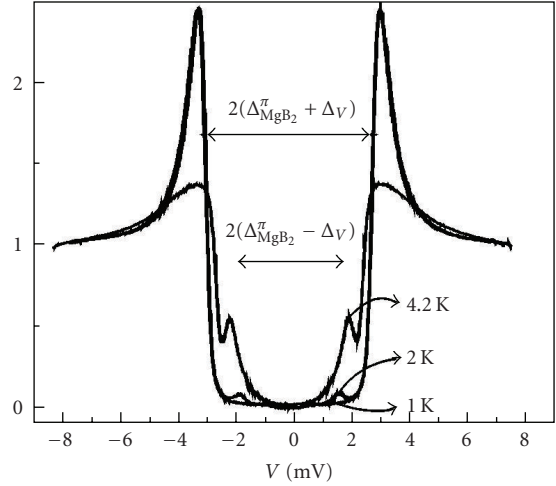


FIGURE 5: (From [26]) Normalized differential conductance of a MgB₂/Al₂O₃/V tunnel junction, showing evidence for sum and difference gaps of the two superconductors. © American Institute of Physics.

(including spin-polarization studies [29–31]) but also are the precursor to highly applicable Josephson junctions. Josephson tunneling is achieved when paired electrons (a super-current) tunnel through the insulator while remaining paired, thus without any voltage drop. This process is extremely sensitive to electromagnetic flux, thus making Josephson junctions the central component of numerous highly sensitive detectors [32, 33].

Using MBE-grown MgB₂ coupled with a traditional low-temperature superconductor such as vanadium, Kim and Moodera [26, 34] successfully demonstrated all in situ thin film tunnel junctions. Following the growth of MgB₂ on Si (with the MgO buffer as described above), a thin layer of Al₂O₃ was formed by oxidizing an ultra thin film of Al, and finally V cross-strips were deposited. Traditional four terminal transport measurements at 4.2 K and 1 K of such MgB₂/Al₂O₃/V junctions revealed the typical superconductor-insulator-superconductor (SIS) quasiparticle tunneling behavior, with a clear superconducting gap structure emerging. Sum and difference gaps of the two top and bottom superconductor electrodes were clearly observed as expected, and shown in Figure 5. The superconducting gap values at 2 K for the two electrodes were found to be 2.4 meV and 0.7 meV for MgB₂ (π -gap) and V, respectively. This yielded a reduced BCS ratio of 1.5 for the MgB₂, showing weakly coupled superconductivity. At lower temperatures, for measurements taken at 0.45 K, additional features appeared in the conductance curve at values near 6.8 meV, corresponding to the MgB₂ σ -gap, shown in Figure 6. The BCS ratio in this case is 4.25, a signature of strongly coupled superconductivity. Such experiments were repeated using MgO as a tunneling barrier, and the good tunneling behavior was reproduced. By reducing the thickness of the tunneling barrier, Kim and Moodera [26, 34] were able to observe Josephson tunneling in MgB₂/Al₂O₃/V and MgB₂/MgO/V junctions (inset in Figure 6).

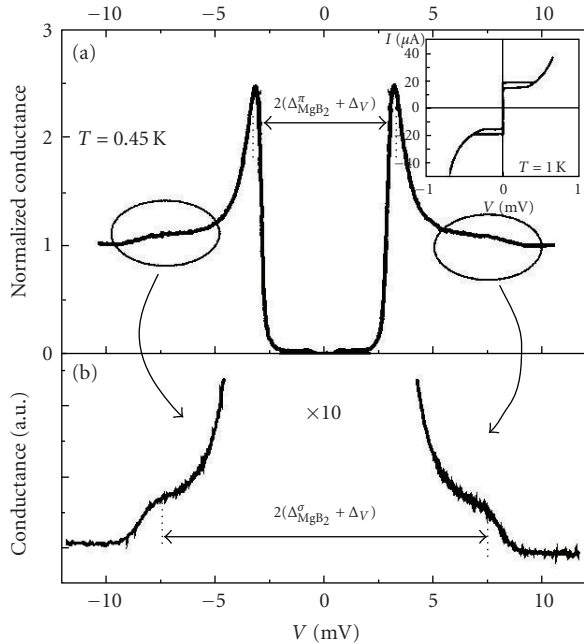


FIGURE 6: (From [26]) Tunneling characteristics of a $\text{MgB}_2/\text{Al}_2\text{O}_3/\text{V}$ tunnel junction at 0.45 K, showing σ -gap tunneling features. *Inset:* Josephson pair tunneling occurs with a thinner barrier. © American Institute of Physics.

The demonstration of clean quasiparticle and pair tunneling through an MgO barrier is significant, as it opens the possibility of using another layer of epitaxial MgB_2 , grown on top of the oriented barrier, as a top electrode. The MBE deposition method indeed allows for such all- MgB_2 junctions structures to be formed without breaking the vacuum. Such junctions would be a great implementation and use of MgB_2 's properties, completely eliminating the need for liquid He-based cooling, and benefiting from the fast operation speed possible due to the large energy gap. Kim and Moodera [34] realized such junctions in 2006, by successive deposition of MgB_2 , MgO, and MgB_2 . It is notable here that the top electrode could be of high crystalline quality for optimal device operation. Due to the nature of growth, it is unavoidable that the interface between the barrier and the top electrode would be rougher than those interfaces closer to the substrate. The effect of this was shown in the reduced T_C of 28 K for the top MgB_2 , still a significant improvement over traditional low-temperature superconductors. Nonetheless, significant Josephson tunneling current was observed up to 25 K, and these junctions had an $I_C R_N$ product of ~ 4 meV. The $I_C R_N$ product (of the critical current I_C and the normal state resistance R_N) being so high and close to the π -gap value is a huge benefit for potential high-speed electronics applications. It is also noteworthy that it is relatively easier to form sandwich type junctions with MgB_2 compared to most of the oxide high- T_C materials [35].

The lateral size of Josephson junction stacks is essential when considering the effect of electromagnetic fields on Josephson signals. For the case of magnetic fields, it is well

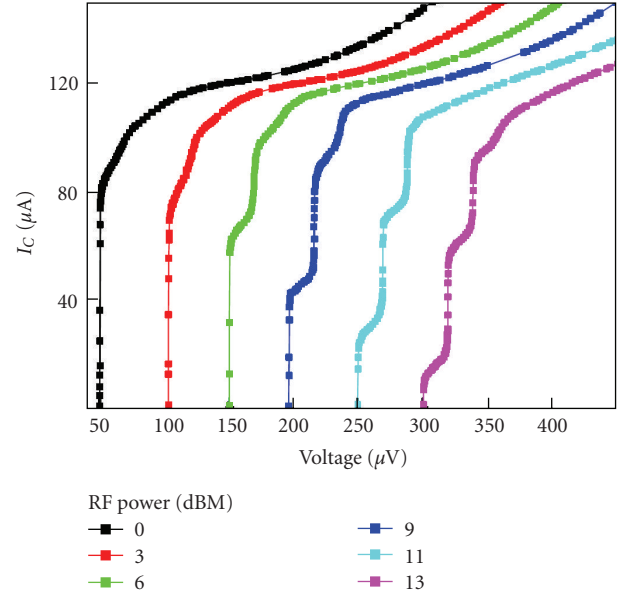


FIGURE 7: (From [27]) Current-voltage characteristics of an all- MgB_2 tunnel junction with an MgO barrier, under different RF irradiation power. The junction size is $60 \times 60 \mu\text{m}^2$. The curves are horizontally shifted for clarity. © American Institute of Physics.

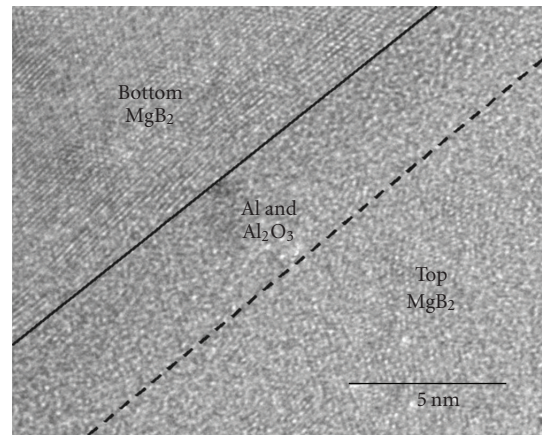


FIGURE 8: (From [28]) Cross-sectional TEM image of an all- MgB_2 junction with an Al_2O_3 barrier. The bottom electrode is crystalline, whereas the barrier and top electrode are clearly randomly oriented. © American Institute of Physics.

established that the phase of the Josephson current is linked to the total flux through the junction. At small enough junction sizes the current density through the entire area of the junction is uniform, and the maximum Josephson current, the critical current, follows the Fraunhofer diffraction pattern, [24, 32, 36]. Similarly, microwave irradiation of a Josephson junction affects the critical current, with radio-frequency (RF) power causing distinctive Shapiro steps in the current-voltage measurements [27, 32, 37].

Costache and Moodera [28] deposited all MgB_2 -based tunnel junctions by MBE, with an MgO tunnel barrier, similarly to the work described above. However in this case,

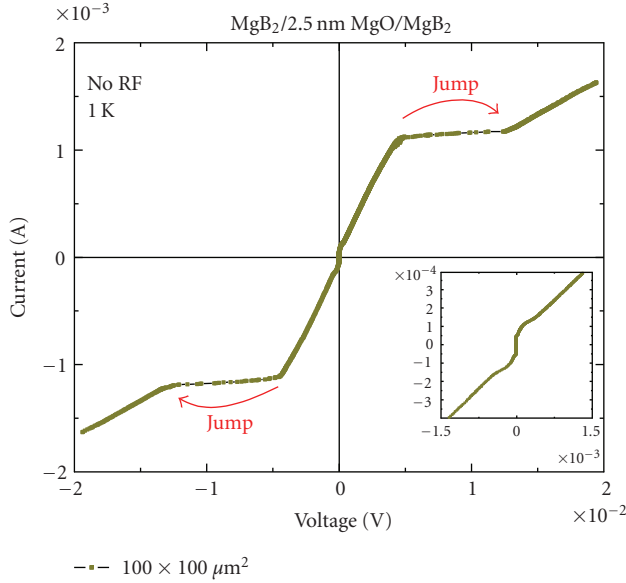


FIGURE 9: Current-voltage measurement for an all-MgB₂ junction with a sputtered MgO barrier. The data was collected in constant-current mode. The jump occurring at ± 12.7 mV corresponds to tunneling between the MgB₂ σ -gaps.

instead of shadow masking during deposition, the films were postpatterned using standard optical lithography, so that junctions with lateral dimensions down to $20 \times 20 \mu\text{m}^2$ could be formed. The width of the junctions being smaller than four-times the Josephson penetration depth, these could be considered in the small junction limit. Despite the lithography and processing possibly damaging the superconducting thin films—the top electrode in particular—Josephson tunneling was observed in such devices up to 21 K. A thickness of 2.4 nm (as measured by quartz microbalance crystal during deposition) for the MgO barrier was determined as optimal for pair tunneling. This value was established as a tradeoff between leakage from sub-gap conductance for junctions with thinner MgO barriers, and quasiparticle tunneling dominated transport for thicker barrier junctions. The ac Josephson effect was measured for these junctions at 4.2 K and under RF irradiation of 9.3 GHz, and Costache and Moodera [28] observed clear Shapiro steps appearing as the excitation power was increased, as shown in Figure 7. The occurrence of the Shapiro steps follow the expected voltage position values at with $V = nhf/2e$, with n an integer, f the excitation frequency, h and e Planck's constant and the electron charge, respectively. Potential issues with magnetic flux trapping in the MgB₂, however, meant the critical current variation following the Fraunhofer diffraction pattern could not be observed in these junctions. Concerns thus may arise in these measurements as to the role of any leakage current in addition to the Josephson current. The Fraunhofer diffraction pattern has been shown by others in MgB₂-based junctions [24, 36].

Exploration of the dual-gap nature of MgB₂ has also yielded promising results. As mentioned above, the very large σ -gap with a value of 7.1 meV is potentially very useful for

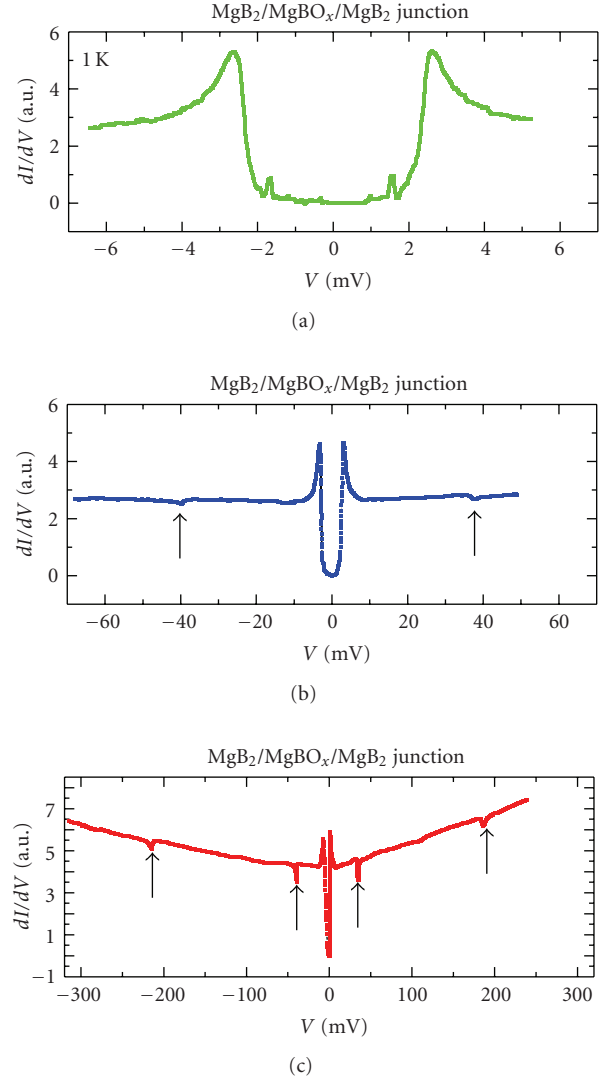


FIGURE 10: Tunneling characteristics of a MgB₂/MgBO_x/MgB₂ tunnel junction. The dips in the conductance curve correspond to phonon interactions in the barrier.

high-speed electronics. The proportion of transport through either or both of the two gaps is a function of the crystal direction, with π -gap transport dominant in the c -axis direction, and σ -gap dominant for the case of transport in the a - b plane. In order to study the properties of the σ -gap, Shim et al. [38] moved away from textured MgO barriers and studied all-MgB₂ junctions with polycrystalline Al₂O₃ tunnel barriers. This would then cause a loss of orientation in the top superconductor, thus exposing potentially all crystal directions to the vertical current flow. XRD and cross-sectional transmission electron microscopy (TEM) confirmed that while the bottom electrode (grown on the MgO buffer) was epitaxial, the top MgB₂ was randomly oriented, shown in Figure 8. It was also found that the T_C of thin films grown on Al₂O₃ was up to 10 K lower than identical films grown on MgO, for a range of MgB₂ thicknesses. Quasi-particle transport measurements taken

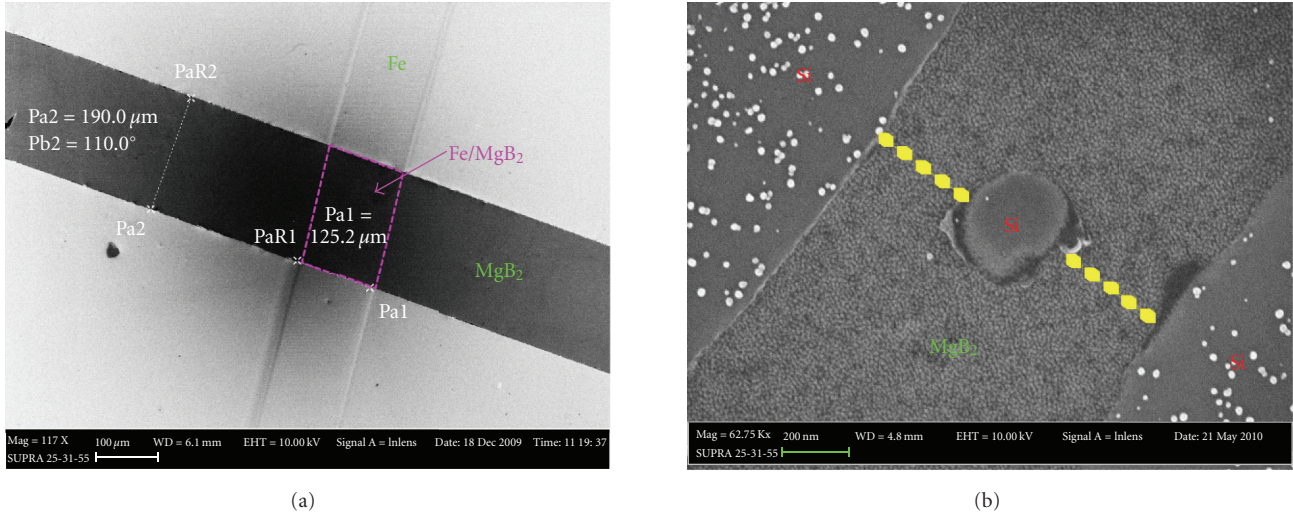


FIGURE 11: Scanning electron microscopy images of possible thin film MgB_2 devices: (a) weak link created by Fe proximity effect; (b) superconducting quantum interference device geometry, where the two yellow dashed lines would be Josephson junctions.

on junctions formed with the Al_2O_3 tunnel barrier indeed revealed clear σ -gap tunneling features associated with the top layer.

Another approach to deposition of a robust tunneling barrier is sputtering. Sputtering can potentially yield a thin very homogeneous barrier without the experimental drawbacks of MBE. It is noteworthy that without a high-temperature postanneal it is unlikely that a sputtered barrier will be oriented. Using the same MgB_2 deposition method as previously discussed, we have explored sputtered MgO as a tunnel barrier for quasiparticle and Josephson junctions. Quasi-particle or Josephson tunneling was successfully observed, depending on the thickness of the barrier. An example current-voltage characteristics with an MgO barrier 2.5 nm thick in an all MgB_2 junction is shown in Figure 9. This data was collected in constant-current mode, and displays two notable features: a small zero-voltage current, sustained briefly, and a jump to a resistive tunneling regime above 12.7 mV. This latter behavior indicates a superconducting gap, and corresponds to transport between the σ -bands of the two electrodes. The top electrode once again has a slightly reduced gap value as compared to the bottom electrode grown on the crystalline MgO buffer layer. Thus, in these junctions, roughness at the interfaces with the barrier and the fact that the sputtered barrier provides excellent coverage of this roughness can lead to in-plane tunneling channels to exist. These horizontal channels will also have an effectively reduced thickness as compared to the traditional vertical tunneling direction, explaining their prevalence in the measurements.

Until now, we have been mentioning MgO and MgB_2 in the same devices, but not in an interacting manner. The Mg content in both is a natural link between these two materials, and leads us to yet another possibility for a tunnel barrier, that of the natural oxide MgBO_x . It is possible to oxidize the surface of MgB_2 in a controlled manner using O_2 exposure or a glow discharge plasma, both within the

growth chamber, to form tunnel junctions with an MgBO_x barrier. Although Josephson junctions were not formed with this barrier, quasiparticle tunneling and the superconducting gap were observed. Example differential conductance curves are shown in Figure 10 for a selection of bias voltage ranges. The barrier thickness as fitted to the current-voltage curve was found to be 2.1 nm, with a barrier height of 1.32 eV. The fact that tunneling and the superconducting gap features were observed is an encouraging indication that barriers formed directly by oxidation of MgB_2 might be viable and easy route for future devices. Singh et al. [39] also explored MgB_2 -based junctions formed using the native oxide as the insulating barrier. The oxide was formed by exposing the MBE-grown films to ambient atmosphere at room temperature or at 160°C for one hour. They were able to detect gap features in the transport characteristics of such junctions at temperatures up to 30 K, and had pinhole-free barriers for areas larger than 1 mm^2 . Although the exact chemistry of the barrier is difficult to determine, and depends on the surface stoichiometry, this again demonstrates that natural oxide barriers are a promising and robust candidate for future implementation. More recently, Shen et al. [40] were able to form Josephson junctions by pressing together two oxidized MgB_2 thin films.

Planar or edge junctions using a thin film of MgB_2 have also been formed and studied [41, 42]. In these devices, one side of the superconducting film is removed, and a tunnel barrier and second superconducting electrode are then deposited, so that they overlap the step region in the MgB_2 . This has one clear experimental advantage which is that one lateral dimension of the junction area is determined by the thickness of the original film, thus can be reliably determined to be in the nanometer size regime. In addition, these junctions allow the direct probing of in-plane a - b plane transport, and thus the σ -gap of MgB_2 . In one case using these types of junctions, Brinkman et al. [41] observe a sharp peak in the spectra, possibly corresponding to Leggett

mode resonance [42]. This was predicted for multigap superconductors as a manifestation of the relative phase of the π and σ condensates, and MgB_2 is an ideal candidate to further explore this.

Inspired by previous work on the traditional elemental superconductors, one can transfer those ideas, and imagine a multitude of others, which can be fruitfully applied to MgB_2 . Particularly, the probing of the large σ -gap using lateral junctions is of great research interest with applications in mind. One such lateral junction geometry uses the deposition of a ferromagnetic material, for example, Fe, locally on superconducting channels. By proximity, this will destroy superconductivity in the MgB_2 in contact with Fe. Another approach is to constrict very thin MgB_2 channels, to again induce a nonsuperconducting segment to act as a normal metal barrier. Once this is achieved reliably, one can imagine a near-total break in the MgB_2 channel could act as a tunneling barrier. Developing on this further, a thin film of MgB_2 may be patterned directly into a superconducting quantum interference device by creating a flux penetration loop directly in the film. Examples of development devices for some of these ideas are shown in Figure 11. In fact, with this robust material, one should be able to pattern an entire circuit incorporating junctions, detectors and other components directly into a film.

Moving away from traditional tunnel junctions, MgB_2 offers the potential for good insight and novel devices. For instance, point contact spectroscopy can be used to detect conductance in the sub-gap region due to the occurrence of Andreev reflection. According to recent theories, in a multiband superconductor like MgB_2 , interference can exist between different conduction channels. The multiband Blonder-Tinkham-Klapwijk model with interference effects included is now available and makes experimental investigation of such phenomena very valuable. Epitaxial MgB_2 thin films are an ideal prototype system for multiband superconductivity [43, 44].

Overall, while concentrating on thin film junctions formed in situ, we have seen that MgB_2 holds great promise for the implementation of devices and detectors [23, 45–48]. The interest naturally begins with the material; the relatively high T_C and availability of Mg and B mean that MgB_2 is an ideal candidate for applications ranging from high-field magnet coils to single-photon detectors. Only one decade has passed since the discovery of its superconductivity, but already MgB_2 has generated terrific research in institutes and industries all over the world, and it is clear that its potential has not yet been fully met.

Acknowledgment

The authors acknowledge support from the Office of Naval Research under Grant numbers N00014-02-1-0119 and N00014-06-1-0235.

References

- [1] J. Nagamatsu, N. Nakagawa, T. Muranaka, Y. Zenitani, and J. Akimitsu, "Superconductivity at 39 K in magnesium diboride," *Nature*, vol. 410, no. 6824, pp. 63–64, 2001.

- [2] R. Musenich, P. Fabbriatore, S. Farinon et al., "The behaviour of cryogen-free MgB_2 react and wind coils," *Superconductor Science and Technology*, vol. 19, no. 3, pp. S126–S131, 2006.
- [3] X. H. Li, X. J. Du, M. Qiu, Y. W. Ma, and L. Y. Xiao, "Design and experimental demonstration of an MgB_2 based 1.5 T MRI test magnet," *Physica C*, vol. 463–465, pp. 1338–1341, 2007.
- [4] W. Yao, J. Bascuñán, W. S. Kim, S. Hahn, H. Lee, and Y. Iwasa, "A solid nitrogen cooled MgB_2 "demonstration" coil for MRI applications," *IEEE Transactions on Applied Superconductivity*, vol. 18, no. 2, pp. 912–915, 2008.
- [5] A. Y. Liu, I. I. Mazin, and J. Kortus, "Beyond Eliashberg superconductivity in MgB_2 : anharmonicity, two-phonon scattering, and multiple gaps," *Physical Review Letters*, vol. 87, no. 8, Article ID 087005, 4 pages, 2001.
- [6] F. Giubileo, D. Roditchev, W. Sacks et al., "Two-gap state density in MgB_2 : a true bulk property or a proximity effect?" *Physical Review Letters*, vol. 87, no. 17, Article ID 177008, 4 pages, 2001.
- [7] I. I. Mazin, O. K. Andersen, O. Jepsen et al., "Superconductivity in MgB_2 : clean or dirty?" *Physical Review Letters*, vol. 89, no. 10, Article ID 107002, 4 pages, 2002.
- [8] H. J. Choi, D. Roundy, H. Sun, M. L. Cohen, and S. G. Louie, "The origin of the anomalous superconducting properties of MgB_2 ," *Nature*, vol. 418, no. 6899, pp. 758–760, 2002.
- [9] I. I. Mazin and V. P. Antropov, "Electronic structure, electron-phonon coupling, and multiband effects in MgB_2 ," *Physica C*, vol. 385, no. 1-2, pp. 49–65, 2003.
- [10] V. Moshchalkov, M. Menghini, T. Nishio et al., "Type-1.5 superconductivity," *Physical Review Letters*, vol. 102, no. 11, Article ID 117001, 2009.
- [11] M. R. Eskildsen, M. Kugler, S. Tanaka et al., "Vortex imaging in the π band of magnesium diboride," *Physical Review Letters*, vol. 89, no. 18, Article ID 187003, 4 pages, 2002.
- [12] W. N. Kang, H. J. Kim, E. M. Choi, C. U. Jung, and S. I. Lee, " MgB_2 superconducting thin films with a transition temperature of 39 kelvin," *Science*, vol. 292, no. 5521, pp. 1521–1523, 2001.
- [13] C. B. Eom, M. K. Lee, J. H. Choi et al., "High critical current density and enhanced irreversibility field in superconducting MgB_2 thin films," *Nature*, vol. 411, no. 6837, pp. 558–560, 2001.
- [14] M. Paranthaman, C. Cantoni, H. Y. Zhai et al., "Superconducting MgB_2 films via precursor postprocessing approach," *Applied Physics Letters*, vol. 78, no. 23, pp. 3669–3671, 2001.
- [15] D. H. A. Blank, H. Hilgenkamp, A. Brinkman, D. Mijatovic, G. Rijnders, and H. Rogalla, "Superconducting Mg-B films by pulsed-laser deposition in an in situ two-step process using multicomponent targets," *Applied Physics Letters*, vol. 79, no. 3, pp. 394–396, 2001.
- [16] S. H. Moon, J. H. Yun, H. N. Lee et al., "High critical current densities in superconducting MgB_2 thin films," *Applied Physics Letters*, vol. 79, no. 15, pp. 2429–2431, 2001.
- [17] A. Berenov, Z. Lockman, X. Qi et al., "Growth of strongly biaxially aligned MgB_2 thin films on sapphire by postannealing of amorphous precursors," *Applied Physics Letters*, vol. 79, no. 24, pp. 4001–4003, 2001.
- [18] S. D. Bu, D. M. Kim, J. H. Choi et al., "Synthesis and properties of c-axis oriented epitaxial MgB_2 thin films," *Applied Physics Letters*, vol. 81, no. 10, Article ID 1851, 3 pages, 2002.
- [19] K. Ueda and M. Naito, "As-grown superconducting MgB_2 thin films prepared by molecular beam epitaxy," *Applied Physics Letters*, vol. 79, no. 13, pp. 2046–2048, 2001.
- [20] W. Jo, J. U. Huh, T. Ohnishi, A. F. Marshall, M. R. Beasley, and R. H. Hammond, "In situ growth of superconducting

- MgB₂ thin films with preferential orientation by molecular-beam epitaxy,” *Applied Physics Letters*, vol. 80, no. 19, Article ID 3563, 3 pages, 2002.
- [21] X. Zeng, A. V. Pogrebnaykov, A. Kotcharov et al., “In situ epitaxial MgB₂ thin films for superconducting electronics,” *Nature Materials*, vol. 1, no. 1, pp. 35–38, 2002.
- [22] J. Rowell, “Magnesium diboride: superior thin films,” *Nature Materials*, vol. 1, no. 1, pp. 5–6, 2002.
- [23] X. X. Xi, “Two-band superconductor magnesium diboride,” *Reports on Progress in Physics*, vol. 71, no. 11, Article ID 116501, 2008.
- [24] Y. Cui, K. Chen, Q. Li, X. X. Xi, and J. M. Rowell, “Degradation-free interfaces in MgB₂/insulator/Pb Josephson tunnel junctions,” *Applied Physics Letters*, vol. 89, no. 20, Article ID 202513, 3 pages, 2006.
- [25] A. J. M. Van Erven, T. H. Kim, M. Muenzenberg, and J. S. Moodera, “Highly crystallized as-grown smooth and superconducting MgB₂ films by molecular-beam epitaxy,” *Applied Physics Letters*, vol. 81, no. 26, pp. 4982–4984, 2002.
- [26] T. H. Kim and J. S. Moodera, “Demonstration of all in situ magnesium diboride superconductor thin-film tunnel junctions,” *Applied Physics Letters*, vol. 85, no. 3, pp. 434–436, 2004.
- [27] G. Carapella, N. Martucciello, G. Costabile, C. Ferdeghini, V. Ferrando, and G. Grassano, “Nb/AlO/Al/MgB₂ large area thin films heterostructures: possible observation of tunneling from both dirty and clean limit MgB₂,” *International Journal of Modern Physics B*, vol. 17, no. 4–6, pp. 751–756, 2003.
- [28] M. V. Cosatche and J. S. Moodera, “All magnesium diboride Josephson junctions with MgO and native oxide barriers,” *Applied Physics Letters*, vol. 96, no. 8, Article ID 082508, 3 pages, 2010.
- [29] L. Solymar, *Superconductive Tunneling and Applications*, Wiley-Interscience, New York, NY, USA, 1972.
- [30] E. L. Wolf, *Principles of Electron Tunneling Spectroscopy*, Oxford University Press, New York, NY, USA, 1985.
- [31] J. S. Moodera and G. Mathon, “Spin polarized tunneling in ferromagnetic junctions,” *Journal of Magnetism and Magnetic Materials*, vol. 200, no. 1, pp. 248–273, 1999.
- [32] C. Poole, H. A. Farach, and R. J. Creswick, *Superconductivity*, Academic Press, San Diego, Calif, USA, 1995.
- [33] T. V. Duzer and C. W. Turner, *Principles of Superconductive Devices and Circuits*, Prentice Hall, Upper Saddle River, NJ, USA, 1998.
- [34] T. H. Kim and J. S. Moodera, “Magnesium diboride superconductor thin film tunnel junctions for superconductive electronics,” *Journal of Applied Physics*, vol. 100, no. 11, Article ID 113904, 2006.
- [35] M. Naito, H. Yamamoto, and H. Sato, “Intrinsic problem of cuprate surface and interface: why good tunnel junctions are difficult to fabricate,” *Physica C*, vol. 335, no. 1, pp. 201–206, 2000.
- [36] K. Ueda, S. Saito, K. Semba, T. Makimoto, and M. Naito, “All-MgB₂ Josephson tunnel junctions,” *Applied Physics Letters*, vol. 86, no. 17, Article ID 172502, 3 pages, 2005.
- [37] R. Gonnello, A. Calzolari, D. Daghero et al., “Josephson effect in MgB₂ break junctions,” *Physics Review Letters*, vol. 87, no. 9, Article ID 097001, 2001.
- [38] H. Shim, K. S. Yoon, J. S. Moodera, and J. P. Hong, “All MgB₂ tunnel junctions with Al₂O₃ or MgO tunnel barriers,” *Applied Physics Letters*, vol. 90, no. 21, Article ID 212509, 3 pages, 2007.
- [39] R. K. Singh, R. Gandikota, J. Kim, N. Newman, and J. M. Rowell, “MgB₂ tunnel junctions with native or thermal oxide barriers,” *Applied Physics Letters*, vol. 89, no. 4, Article ID 042512, 2006.
- [40] Y. Shen, R. K. Singh, S. Sanghavi et al., “Characterization of Josephson and quasi-particle currents in MgB₂ /MgB₂ and Pb/Pb contact junctions,” *Superconductor Science and Technology*, vol. 23, no. 7, Article ID 075003, 2010.
- [41] A. Brinkman, S. H. W. Van Der Ploeg, A. A. Golubov, H. Rogalla, T. H. Kim, and J. S. Moodera, “Charge transport in normal metal-magnesiumdiboride junctions,” *Journal of Physics and Chemistry of Solids*, vol. 67, no. 1–3, pp. 407–411, 2006.
- [42] A.J. Leggett, “Number-phase fluctuations in two-band superconductors,” *Progress of Theoretical Physics*, vol. 36, pp. 901–930, 1966.
- [43] A. A. Golubov, A. Brinkman, Y. Tanaka, I. I. Mazin, and O. V. Dolgov, “Andreev spectra and subgap bound states in multiband superconductors,” *Physical Review Letters*, vol. 103, no. 7, Article ID 077003, 2009.
- [44] W. K. Park and L. H. Greene, “Andreev reflection and order parameter symmetry in heavy-fermion superconductors: the case of CeCoIn,” *Journal of Physics Condensed Matter*, vol. 21, no. 10, Article ID 103203, 2009.
- [45] S.-W. Cheong and N. Hur, “MgB₂ superconductors,” U.S. Patents no. 7,668,578, 2004.
- [46] T. G. Ference and K. A. Puzey, “Method of increasing the critical temperature of a high critical temperature superconducting film and a superconducting structure made using the method,” U.S. Patents no. 6,630,426, 2000.
- [47] H. Shim and J. S. Moodera, “Josephson junction device for superconductive electronics with a magnesium diboride,” U.S. Patents no. 7,741,634, 2008.
- [48] M. Katagiri and M. Ohkubo, “Methods for detecting photons, radiations or neutrons using superconductors and methods for obtaining two-dimensional images thereof,” U.S. Patents no. 7,030,379, 2006.



Hindawi

Submit your manuscripts at
<http://www.hindawi.com>

